

Synthesis and Structure of New Cd–Bi–S Homologous Series: A Study in Intergrowth and the Control of Twinning Patterns

Wonyoung Choe, Stephen Lee,* Patrick O'Connell, and Aaron Covey

Department of Chemistry, The University of Michigan, Ann Arbor, Michigan 48109-1055

Received May 23, 1997. Revised Manuscript Received July 14, 1997[Ⓢ]

Four compounds, CdBi_2S_4 , CdBi_4S_7 , $\text{Cd}_{2.8}\text{Bi}_{8.1}\text{S}_{15}$, and $\text{Cd}_2\text{Bi}_6\text{S}_{11}$, have been synthesized using a RbCl/LiCl flux. Single-crystal X-ray structure refinements were made for CdBi_2S_4 and $\text{Cd}_{2.8}\text{Bi}_{8.1}\text{S}_{15}$. The final R values for these two crystals were respectively 3.05% and 5.53%. The compounds CdBi_2S_4 and CdBi_4S_7 are isotypic with respectively HgBi_2S_4 and Y_5S_7 . $\text{Cd}_{2.8}\text{Bi}_{8.1}\text{S}_{15}$ can be considered as an ordered intergrowth between the two phases CdBi_2S_4 and CdBi_4S_7 and belongs to a new structure type as does $\text{Cd}_2\text{Bi}_6\text{S}_{11}$. All four structures can be viewed as chemically twinned NaCl superstructures where the twinning plane is the (113) plane. We find there is segregation of the larger Bi atoms toward the twinning planes, whereas smaller Cd atoms occupy the interior sites of the NaCl domain. We also find that the average oxidation state of the cations controls the twinning patterns even in the presence of metal disorder. We propose the possible twinning patterns for $\text{Cd}_2\text{Bi}_6\text{S}_{11}$ based on the observed average oxidation state of metal cations. The space groups of CdBi_2S_4 , CdBi_4S_7 , and $\text{Cd}_{2.8}\text{Bi}_{8.1}\text{S}_{15}$ are $C2/m$ for all three crystals. Cell axes for the three phases are respectively $a = 13.095(2)$ Å, $b = 3.9792(7)$ Å, $c = 14.611(3)$ Å, $\beta = 116.30(1)^\circ$; $a = 13.112(2)$ Å, $b = 4.0032(7)$ Å, $c = 11.765(2)$ Å, $\beta = 105.21(1)^\circ$; and $a = 13.111(2)$ Å, $b = 3.9885(8)$ Å, $c = 24.710(5)$ Å, $\beta = 97.84(2)^\circ$. Cell axes for $\text{Cd}_2\text{Bi}_6\text{S}_{11}$ are $a = 13.112(3)$ Å, $b = 3.997(1)$ Å, $c = 35.84(1)$ Å, and $\beta = 90.39(2)^\circ$.

Introduction

One recent theme in crystal chemistry is the interplay between crystalline defects and extended superstructures.^{1a} Planar extended defects in the twinned crystals form tilt planes. Chemists as well as mineralogists refer to the formation of these tilt planes as chemical twinning.^{1b} Chemical twinning of many sulfides and mineral sulfosalts has been extensively studied as it allows one to use this concept to build a complex superstructure from simple structural units. For example, the mineral ourayite, $\text{Ag}_{25}\text{Pb}_{30}\text{Bi}_{41}\text{S}_{104}$, adopts the crystal structure shown in Figure 1.^{1c} As this figure illustrates, a simple twinning operation in the crystal-lites creates an interplanar separation of 22 Å between the tilt planes. Ourayite contains rock salt crystallites that form (113) symmetrical twin planes and therefore belongs to a general family of (113) plane twinned ordered crystalline phases. This main family includes both the lillianite and pavonite homologous series.¹ Members of this family include numerous phases from the Pb–Bi–S, Ag–Pb–Bi–S, Cu–Bi–S, Mn–Y–S, and Mn–Er–S families, as well as other ternary, quaternary, and even higher bismuth sulfides. In all cases, it

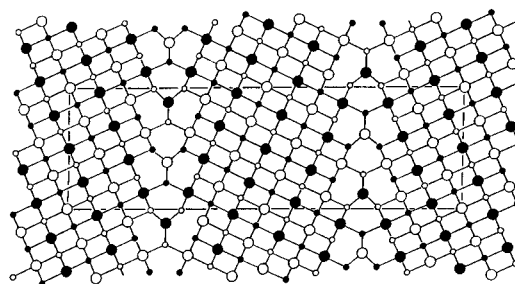


Figure 1. Crystal structure of ourayite ($\text{Ag}_{25}\text{Pb}_{30}\text{Bi}_{41}\text{S}_{104}$), one of the lillianite homologues. The open and closed circles are respectively at $z = 0$ and $z = 0.5$. The small and large circles correspond respectively to sulfur and metal atoms.

is known that the excess of sulfur atoms over metal atoms controls the number of (113) symmetrical tilt planes.^{1b} A striking feature of these homologous series is the fact that these materials can accommodate the change in cation-to-anion ratio by changing the repetition of twinning planes and such variation could produce desired physical characteristics such as thermoelectric power^{2a} and bandgap energy.^{2b–d} In this paper we study

* To whom correspondence should be addressed.

[Ⓢ] Abstract published in *Advance ACS Abstracts*, September 1, 1997.

(1) (a) Hyde, B. G.; Andersson, S. *Inorganic Crystal Structures*; Wiley: New York, 1989. (b) Hyde, B. G.; Andersson, S.; Bakker, M.; Plug, C. M.; O'Keeffe, M. *Prog. Solid State Chem.* **1980**, *12*, 273. (c) Makovicky, E.; Karup-Møller, S. *N. Jb. Miner. Abh.* **1977**, *130*, 264; **1977**, *131*, 56. (d) Otto, H. H.; Strunz, H. *N. Jb. Miner. Abh.* **1968**, *108*, 1. (e) Takéuchi, Y.; Takagi, J. *Proc. Jpn. Acad. Sci.* **1974**, *50*, 843. (f) Makovicky, E. *Fortschr. Miner.* **1981**, *59*, 137. (g) Tilley, R. J. D.; Wright, A. C. *J. Solid State Chem.* **1986**, *65*, 45. (h) Colaitis, D.; van Dyck, D.; Amelinckx, S. *Phys. Status Solidi* **1981**, *68*, 419. (i) Takéuchi, Y.; Takagi, J.; Yamanaka, T. *Z. Kristall.* **1974**, *140*, 249. (j) Landa-Canovas, A. R.; Otero-Diaz, L. C. *Aust. J. Chem.* **1992**, *45*, 147.

(2) Bismuth chalcogenide compounds draw considerable attention recently due to potential application as thermoelectric materials. See: (a) Kanatzidis, M. G.; McCarthy, T. J.; Tanzer, T. A.; Chen, L.-H.; Iordanidis, L.; Hogan, T.; Kannewurf, C. R.; Uher, C.; Chen, B. *Chem. Mater.* **1996**, *8*, 1465. CdS and Bi_2S_3 are two important members of semiconducting chalcogenides for solar cell application because their bandgap energies are similar to that of the sun light. See: (b) Misra, S.; Padhi, H. C. *J. Appl. Phys.* **1994**, *75*, 4576. (c) Lokhande, C. D.; Yermune, V. S.; Pawar, S. H. *J. Electrochem. Soc.* **1991**, *138*, 624. These authors reported the bandgap of the solid solution of $\text{CdS-Bi}_2\text{S}_3$ thin films. However, to our best knowledge, no single-crystal structure study has been conducted on Cd–Bi–S ternary system. See ref 4 for previous works.

Table 1. Microprobe Analysis for Four Cd–Bi–S Phases and Crystallographic Cell Constants

compound	microprobe analysis	X-ray refinement	<i>a</i> (Å)	<i>b</i> (Å)	<i>c</i> (Å)	β (deg)
CdBi ₄ S ₇	Cd _{0.0861(1)} Bi _{0.326(2)} S _{0.586(2)}		13.112(2)	4.0032(7)	11.765(2)	105.21(1)
Cd ₂ Bi ₆ S ₁₁	Cd _{0.108(2)} Bi _{0.318(6)} S _{0.574(7)}		13.112(3)	3.997(1)	35.84(1)	90.39(2)
Cd _{2.8} Bi _{8.1} S ₁₅	Cd _{0.111(2)} Bi _{0.303(3)} S _{0.586(4)}	Cd _{0.11} Bi _{0.31} S _{0.58}	13.111(2)	3.9885(8)	24.710(5)	97.84(2)
CdBi ₂ S ₄	Cd _{0.141(1)} Bi _{0.284(1)} S _{0.575(1)}	Cd _{0.14} Bi _{0.29} S _{0.57}	13.095(2)	3.9792(7)	14.611(3)	116.30(1)

these phases from a structural viewpoint. In particular the crystal ordering in the direction perpendicular to the intergrowth plane allows one to characterize the (113)–(113) interface. Interfaces in general form a cornerstone of our understanding of materials science as it is the interface which often controls mechanical and transport properties.³ Our understanding of interfaces is hampered by the great difficulty in well characterizing a general solid–solid interface. Chemically twinned crystals, such as ourayite discussed above, can provide a treasure trove of information about crystal–crystal interfaces especially crystal interfaces based on crystallographic twinning.

In this paper we report the synthesis of four new members of this homologous series: CdBi₂S₄, CdBi₄S₇, Cd_{2.8}Bi_{8.1}S₁₅, and Cd₂Bi₆S₁₁.⁴ Of these CdBi₂S₄ and CdBi₄S₇ are isotypic with previously established structures.⁵ Cd_{2.8}Bi_{8.1}S₁₅ belongs to a new structure type. We also report the single-crystal structures of CdBi₂S₄ and Cd_{2.8}Bi_{8.1}S₁₅. We find that the number of twinned planes, such as they are, is controlled by the average oxidation state of the cations. There is segregation (i.e., the preponderance of certain elements at certain sites) of Bi atoms toward capped trigonal prismatic sites along the (113) plane and these prismatic sites can therefore accommodate larger Bi atoms. There is also a variable amount of segregation of cadmium into the interior of the rock-salt-like layers.

Experimental Section

A series of samples was prepared from mixtures of Cd, Bi, S, RbCl, and LiCl. Nominal purities were Cd 99.5%, Bi 99.9%, S 99.999%, RbCl 99.8%, and LiCl 99+% pure, all from Aldrich. The LiCl and RbCl were first mixed in a 45:55 mole ratio and then melted under flame (nominal mp 312 °C) and left to dry for several minutes under a 10^{−3} Torr vacuum. Cd, Bi, and S were mixed with the composition Cd_xBi_{2x+3}S_{x+3} with *x* varying between 0.45 and 1.10. These initial compositions correspond to having respective oxidation states for the Cd, Bi, and S atoms of +2, +3, and −2. We placed approximate 1-g samples of the combined Cd–Bi–S mixture with 2 g of the RbCl/LiCl flux in vacuum-sealed quartz tubes. All mixtures were heated to 800 °C at 0.5 °C/min, held at this temperature for 4 days,

(3) *Materials Interfaces: Atomic-level structure and properties*; Wolf, D., Yip, S., Eds.; Chapman and Hall: London, 1992.

(4) Previous reports of Cd–Bi–S phases include: (a) Sher, A. A.; Odin, I. N.; Novoselova, A. V. *Russ. J. Inorg. Chem.* **1986**, *31*, 326. These authors found by powder methods three orthorhombic phases with rough stoichiometries of CdBi₂S₄, Cd₂Bi₁₀S₁₇, and Cd₃Bi₁₀S₁₈. For the CdBi₂S₄ phase, for example, a composition which we also found in the current work, the earlier reported cell constants were *a* = 53.30(5) Å, *b* = 13.25(1) Å, and *c* = 4.647(1) Å, quite different from the monoclinic cell reported in the current work. (b) Brouty, C.; Spinat, P.; Herpin, P. *Rev. Chim. Miner.* **1975**, *12*, 60. These authors found powder patterns of three triclinic pseudoorthorhombic phases with rough stoichiometries of CdBi₂S₄, Cd₂Bi₆S₁₁, and Cd₃Bi₁₄S₂₄. The cell volumes of these phases correspond to cells roughly 2 or 4 times bigger than the C-centered monoclinic cell volumes reported in the current work for respectively CdBi₂S₄, Cd_{2.8}Bi_{8.1}S₁₅, and CdBi₄S₇. The close correspondence between the cell volumes in this earlier and the current work demonstrate that the small incorporation of the flux into our single-crystal samples did not alter the overall crystal character.

(5) (a) HgBi₂S₄: Mumme, W. G.; Watts, J. A. *Acta Crystallogr.* **1980**, *B36*, 1300. (b) Y₅S₇: Adolphe, C. *Ann. Chim.* **1965**, *10*, 271.

and then cooled to 400 °C at 2.4 °C/h, at which point they were annealed for 1 or more weeks. At this point the furnace was turned off, and the samples were cooled to room temperature while still in the furnace. The quartz tubes were broken and the product was washed with water and ethanol to remove first salt and then water. Powder X-ray photographs were taken of the products (Enraf-Nonius Guinier camera, Cu K α ₁ radiation, and NIST Si internal standard). We analyzed single crystals by electron microprobe (Camera MBX automated microprobe, WDS for quantitative stoichiometry, and KEVEX EDS for nonstandardized measurements). Standards for WDS measurements were elemental Bi for Bi and CdS for Cd and S. Li and Rb analyses using atomic emission spectroscopy were made on bulk material. Weissenberg (Cu K α radiation) photographs were taken to select crystals for X-ray diffraction data collection. The conditions for the four-circle diffraction data collections are given in the Supporting Information accompanying this paper.

Results

All products reported in this paper had the form of black needles. Despite the uniformity in the appearance of the final products, we were able to identify five different phases including Bi₂S₃. Cell constants for four Cd–Bi–S phases are summarized in Table 1. In the cadmium-rich systems (the most cadmium-rich system had a starting composition of Cd_{1.1}Bi_{2.0}S_{4.1}) the Guinier powder patterns proved to be of a new compound whose pattern resembled that of HgBi₂S₄. For the most cadmium-rich system, all the lines in the Guinier photograph could be indexed to a cell similar to that of HgBi₂S₄, indicating a near quantitative yield of this product. As shown in Table 1 both microprobe analysis on single crystals in this sample and a single-crystal X-ray study confirmed that the product was CdBi₂S₄. By contrast, in the more bismuth-rich systems (the most bismuth-rich mixture had a starting composition of Cd_{0.45}Bi_{2.0}S_{3.45}) we could identify two main products from the Guinier powder patterns. These proved to be Bi₂S₃ and a new compound whose Guinier powder pattern could be indexed to a cell similar to that found for Y₅S₇. The relative intensities of the Guinier powder lines corresponded well with those calculated for a CdBi₄S₇ phase assumed to be isotypic with Y₅S₇.^{5b} The agreement was especially good if we assigned the cadmium atoms to fully occupy the Y1(2a) position and the bismuth atoms to occupy the Y2(4i) and Y3(4i) positions of the Y₅S₇ structure. This indexing of powder lines is given in the Supporting Information. As shown in Table 1, microprobe analysis of the CdBi₄S₇ crystals confirmed this composition. For samples with starting composition of Cd_xBi_{2x+3}S_{x+3} (0.50 ≤ *x* ≤ 1.00), we could confirm the existence of other phases in the Guinier powder patterns. However, we could not index these new products with known structure types. We therefore selected single crystals for a diffractometer based cell constant determination. Two new types of crystals were found from the cell constant determination. Subsequent microprobe analysis proved the compositions to be Cd_{2.8}Bi_{8.1}S₁₅ and Cd₂Bi₆S₁₁. The microprobe analyses on these new phases are also given in

Table 1. Of the two new crystals only the $\text{Cd}_{2.8}\text{Bi}_{8.1}\text{S}_{15}$ crystal was of sufficient quality to warrant a four-circle data collection. In the case of the $\text{Cd}_{2.8}\text{Bi}_{8.1}\text{S}_{15}$ single-crystal microprobe analysis was carried out on the same crystal used in the four-circle diffractometer data collection. Rb and Li analyses on various bulk samples revealed that the contents of respective elements are below 0.03% and 0.07%. Contamination of our samples by the flux is therefore slight.^{4b}

Structure Determination of CdBi_2S_4 . A crystal with dimensions of $0.4 \times 0.05 \times 0.02$ mm was chosen for data set collection. An initial isotropic refinement based on the HgBi_2S_4 structure type where Cd atoms occupied Hg position led to an $R = 8.73\%$ and $wR_2 = 26.22\%$ with 21 parameters.^{6a} However one of the cadmium sites (the final M1 site) had an unusually small thermal factor ($U_{\text{iso}} = 0.008$ vs $U_{\text{iso}} \sim 0.02$ for the other metal sites). We therefore allowed this site to be fully occupied by a statistical mixture of cadmium and bismuth atoms. The refinement led to a roughly equal proportion of cadmium and bismuth at this M1 site, with an $R = 7.35\%$ and $wR_2 = 20.63\%$ for 22 parameters (thermal parameters for two atoms at the M1 site were fixed to the same value). At this point the overall composition appeared to be $\text{Cd}_{0.76}\text{Bi}_{2.24}\text{S}_{4.00}$ in poor agreement either with the microprobe analysis in Table 1 or with the natural oxidation state assignments of +2, +3, and –2 for respectively cadmium, bismuth, and sulfur. We therefore allowed one of the two pure bismuth sites to be partially replaced by cadmium atoms. For one of the two bismuth sites, the final M2 site, this proved to lower the $R = 7.06\%$ and $wR_2 = 19.42\%$ with 23 parameters (thermal parameters for the two atom types at this site were fixed to be equal to one another). The overall stoichiometry at this point was $\text{Cd}_{0.96}\text{Bi}_{2.04}\text{S}_{4.00}$, in reasonable agreement with the microprobe analysis (see Table 1). We then refined the various sites anisotropically. Finally we released all occupation factors except sulfur sites for further refinement. The final occupation factors varied by no more than 1% from the occupation factors of the last isotropic refinement with the exception of Cd3, whose final occupation factor was smaller by 4%. The final composition was calculated to be $\text{Cd}_{0.97}\text{Bi}_{2.01}\text{S}_{4.00}$. Final atomic coordinates and bond distances are given in Tables 2 and 3. The final $R = 3.05\%$ and $wR_2 = 6.60\%$ for 52 parameters. It is of interest that both the microprobe analysis and the single-crystal diffraction results are in agreement with one another (as Table 1 shows in atom percent the microprobe analysis gives $\text{Cd}_{0.141(1)}\text{Bi}_{0.284(1)}\text{S}_{0.575(1)}$ and the single-crystal refinement gives

(6) (a) Refinements were carried out with the Shxl-93 package with refinement against F^2 vs F . For comparative purposes to traditional refinement we report the standard R factor (for reflections where $I > 2\sigma(I)$ as well as wR_2). See: Sheldrick, G. M. *Acta Crystallogr.* **1990**, *A46*, 467. (b) For the $\text{Cd}_{2.8}\text{Bi}_{8.1}\text{S}_{15}$ structure, the anisotropic thermal factor for the S8 atom indicates that the thermal ellipsoid is elongated along the c axis. Many chemically twinned sulfosalts compounds show similar elongated thermal ellipsoid or positional disorder for one of the sulfur atoms. In our review of the literature (see for example ref 1i), we found many previous instances of this distorted thermal ellipsoid. Other examples include (c) $\text{Pb}_{4.65}\text{Bi}_{20.9}\text{S}_{36}$: Takéuchi, Y.; Ozawa, T.; Takagi, J. Z. *Kristall.* **1979**, *150*, 75. (d) $\text{Tm}_{15}\text{S}_{22}$: Zhang, Y.; Franzen, H. F. *J. Less-Common Met.* **1991**, *168*, 377. The $\text{Tm}_{15}\text{S}_{22}$ compound shows similar elongated thermal ellipsoid. The authors reported that the attempt to separate the sulfur position into two with a half occupation failed. We had moved the S8 position of $\text{Cd}_{2.8}\text{Bi}_{8.1}\text{S}_{15}$ structure to the general position but observed no meaningful R factor decrease. We also did not see any superstructure spots on the Weissenberg films of $\text{Cd}_{2.8}\text{Bi}_{8.1}\text{S}_{15}$ samples.

Table 2. Atomic Positions for CdBi_2S_4

atom	x	y	z	occupancy	U_{eq}
M1 ^a	0.0	0.5	0.5000	0.996(11)	0.0201(2)
M2 ^b	0.34978(2)	0.5	0.63291(2)	1.000(9)	0.01716(9)
Bi1	0.71120(2)	0.5	0.85878(2)	0.998(2)	0.01897(9)
Cd1	0.0	0.0	0.0	0.953(4)	0.0218(2)
S1	0.12277(14)	0.5	0.95806(13)	1.0	0.0143(3)
S2	0.16497(14)	0.0	0.55888(14)	1.0	0.0167(3)
S3	0.33027(14)	0.5	0.82246(14)	1.0	0.0163(3)
S4	0.50458(15)	0.0	0.6872(2)	1.0	0.0198(3)

^a M1 is 39.2(4)% Bi and 60.4(7)% Cd. ^b M2 is 82.1(3)% Bi and 17.9(6)% Cd.

Table 3. Interatomic Distances (Å) for CdBi_2S_4

M1	2S4 2.710(2)
	4S2 2.7782(12)
M2	2S4 2.6966(13)
	1S2 2.722(2)
	1S3 2.892(2)
	2S2 2.9436(13)
Bi1	1S1 2.595(2)
	2S3 2.7210(12)
	2S1 2.9821(13)
Cd1	2S3 2.561(2)
	4S1 2.7913(12)

$\text{Cd}_{0.14}\text{Bi}_{0.29}\text{S}_{0.57}$). These results suggest that the actual atom type ratio at the disordered sites may in fact give a fair representation of the actual site disorder. To verify the accuracy of the cadmium and bismuth occupations, we applied the bond valence–bond distance method of Brown et al.^{7,8} In this method one can calculate the expected overall valence of each metal site from knowledge of the metal–sulfur distances and the actual metal type occupying a given site. In the case of statistically disordered sites we used the occupancy weighted average. In particular we found for the M1, M2, Bi1, and Cd1 sites net oxidation states of respectively, 2.7, 3.1, 3.1, and 2.1. The intermediate value of 2.7 corresponds to the 60% Cd/40% Bi site, while the small Cd occupation at the 18% Cd/82% Bi site is too small to detect by the bond valence sum method. These values are in reasonable agreement with both the single-crystal refinement (in sum total) and with the microprobe cadmium and bismuth concentrations.

Structure Determination of $\text{Cd}_{2.8}\text{Bi}_{8.1}\text{S}_{15}$. A crystal with dimensions $0.3 \times 0.05 \times 0.02$ mm was chosen for data set collection. Systematic extinction conditions for the crystal were compatible with space groups $C2/m$, Cm , and $C2$. The R_{merge} 's for all three space groups were comparable, and we therefore refined the structure in $C2/m$, the highest symmetry group of the three. An initial solution based on the Patterson function led to an isotropic refinement where $R = 8.22\%$ and $wR_2 = 24.89\%$ for 40 parameters. The isotropic thermal factors for all sites were approximately equal except for that of the final M1 site which was an order of magnitude smaller than those of the other sites. In analogy to the CdBi_2S_4 refinement, we therefore allowed partial replacement for the cadmium atoms of this site by bismuth atoms. This lowered the R factor to 7.38% and wR_2 to 21.83% for 41 parameters. The stoichiometry at this point was $\text{Cd}_{2.6}\text{Bi}_{8.4}\text{S}_{15.0}$, in only partial agreement with the microprobe analysis.

We therefore examined each of the remaining bismuth sites to see if there was partial occupation of the site

(7) (a) Slupecki, O.; Brown, I. D. *Acta Crystallogr.*, **1982**, *B38*, 1078. (b) Brown, I. D.; Shannon, R. D. *Acta Crystallogr.* **1973**, *A29*, 266. (8) (a) Pauling, L. *J. Am. Chem. Soc.* **1947**, *69*, 542.

Table 4. Atomic Positions for $\text{Cd}_{2.8}\text{Bi}_{8.1}\text{S}_{15}$

atom	<i>x</i>	<i>y</i>	<i>z</i>	occupancy	<i>U</i> _{eq}
M1 ^a	0.5	0.5	0.5	0.99(2)	0.0192(6)
M2 ^b	0.80206(8)	0.5	0.57162(6)	1.000(9)	0.0174(3)
Bi1	0.58384(7)	0.0	0.69350(5)	0.963(4)	0.0182(4)
Bi2	0.56106(7)	0.5	0.84518(6)	0.982(5)	0.0198(4)
Bi3	0.85339(7)	0.5	0.96790(6)	0.964(5)	0.0183(4)
Cd1	0.8223(2)	0.5	0.76736(12)	0.983(7)	0.0232(6)
S1	0.9291(5)	0.5	0.8630(4)	1.0	0.018(2)
S2	0.4621(4)	0.5	0.7456(3)	1.0	0.0146(14)
S3	0.6856(4)	0.0	0.7897(3)	1.0	0.0152(15)
S4	0.3561(4)	0.0	0.4683(4)	1.0	0.020(2)
S5	0.9377(5)	0.0	0.6015(4)	1.0	0.019(2)
S6	0.7159(5)	0.5	0.6726(3)	1.0	0.017(2)
S7	0.7893(5)	0.5	0.0673(3)	1.0	0.018(2)
S8	0.0	0.0	0.0	1.0	0.038(4)

^a M1 is 39.8(7)% Bi and 59.5(11)% Cd. ^b M2 is 82.1(3)% Bi and 17.9(6)% Cd.

Table 5. Interatomic Distances (Å) for $\text{Cd}_{2.8}\text{Bi}_{8.1}\text{S}_{15}$

M1	2S5	2.743(9)
	4S4	2.783(4)
M2	2S5	2.707(5)
	1S4	2.741(9)
Bi1	1S6	2.876(8)
	2S4	2.949(5)
Bi2	1S3	2.562(8)
	2S6	2.736(4)
	2S2	2.956(5)
Bi3	1S2	2.622(8)
	2S1	2.715(4)
Cd1	1S7	2.702(8)
	2S7	2.791(4)
	2S8	2.8081(8)
Cd1	1S1	2.900(8)
	1S6	2.558(8)
	1S1	2.577(9)
	2S3	2.786(4)
	2S2	2.810(4)

by cadmium. We found that only one site (the final M2 site) was potentially defective in bismuth. This site refined to a Bi occupation factor of 90% and a cadmium occupation of 10% with an $R = 7.28\%$ and $wR_2 = 21.54\%$ for 42 parameters. The overall stoichiometry at this point was $\text{Cd}_{2.73}\text{Bi}_{8.27}\text{S}_{15}$. At this point we switched to anisotropic refinement.^{6b} In the final stage we released simultaneously the occupation factor on all metal atom positions. The final $R = 5.53\%$ and $wR_2 = 8.80\%$ for 90 parameters. No metal occupation factor changed by more than 4% from the original isotropic occupation factors. The final stoichiometry is $\text{Cd}_{2.84}\text{Bi}_{8.13}\text{S}_{15}$ in good agreement with both the microprobe analysis in Table 1 ($\text{Cd}_{2.84}\text{Bi}_{7.76}\text{S}_{15}$) and with the assignment of oxidation states of +2, +3, and -2 for respectively cadmium, bismuth and sulfur (i.e., $(2 \times 2.84) + (3 \times 8.13) = 30.07 \approx 30.00 = 2 \times 15$ based on the explicit $\text{Cd}_{2.84}\text{Bi}_{8.13}\text{S}_{15}$ chemical formula). Final atomic coordinates, occupation factors, isotropic thermal factors, and bond distances are given in Tables 4 and 5. Again the good level of agreement between the various sites suggests that the calculated cadmium and bismuth site occupations are a reasonable portrait of the actual atom distribution at the cation sites as in the previous case. The relative cadmium and bismuth distribution may be roughly verified by the bond valence sum rule, as discussed in the previous section. We found for the M1, M2, Bi1, Bi2, Bi3, and Cd1 sites calculated oxidation states of respectively, 2.6, 3.1, 3.1, 2.9, 3.3, and 2.1. The intermediate value of 2.6 corresponds to a 60% Cd/40% Bi

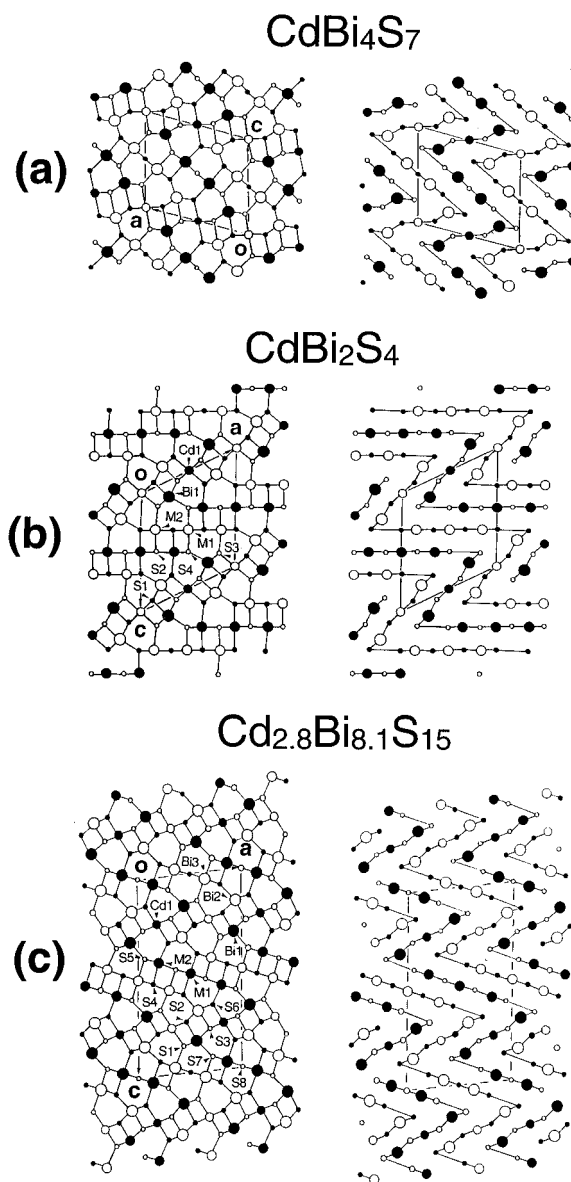


Figure 2. The [010] projections of the $\text{Cd}_x\text{Bi}_2\text{S}_{x+3}$ structures. We emphasize metal-sulfur bonds on the left side of the figures while we show the infinite zigzag line segments on the right. The open and closed circles are respectively at $z = 0$ and $z = 0.5$. (a) The CdBi_4S_7 structure viewed down the [010] axis. CdBi_4S_7 is isotopic with Y_5S_7 structure type and the atomic coordinates were taken from the Y_5S_7 crystal structure.^{5b} This structure has a (4, 3) zigzag sequence. The Y1 site (which is possibly a Cd site in CdBi_4S_7) is located at the origin of the unit cell. See discussion in text. (b) The CdBi_2S_4 structure viewed down the [010] axis. This structure has a (5, 3) zigzag sequence. (c) The $\text{Cd}_{2.8}\text{Bi}_{8.1}\text{S}_{15}$ structure viewed down the [010] axis. This structure has a (5, 3, 4, 3) zigzag sequence.

site. The small occupation of the M2 site by cadmium ($\sim 13\%$) is too small to detect by the bond valence sum method.

Discussion

The compounds CdBi_4S_7 , CdBi_2S_4 , and $\text{Cd}_{2.8}\text{Bi}_{8.1}\text{S}_{15}$ all belong to the same family of chemically twinned cubic closest packed structures. Their crystal structures are illustrated in Figure 2. In Figure 2 we draw these structures from two perspectives. On the left side of this figure we explicitly show the metal-sulfur bonds. Clear from this viewpoint are the narrow slabs of the

Table 6. Calculated and Observed Number of Twinned Planes in Cd–Bi–S Compounds^a

compound	$q/(q-2)$	n
CdBi ₂ S ₄	3.99	4.00
Cd ₃ Bi ₈ S ₁₅	3.73	3.75
Cd ₂ Bi ₆ S ₁₁	3.68	
CdBi ₄ S ₇	3.53	3.50

^a For definitions of q and n see discussion in text.

NaCl structure which appear as ribbons of similarly oriented slightly distorted rectangles. This projected view corresponds to the [110] direction of the original NaCl structure. Each individual NaCl slab is misoriented with respect to its neighbors. These misorientations form a pattern identical with a NaCl (113) tilt plane.

On the right side of Figure 2 we draw these same structures emphasizing that all the atoms in these structures lie in a series of in-tandem zigzag lines. The switches in direction between the zig versus zag parts of the line segments occur at the tilt grain boundaries or chemical twinning planes themselves. For each of the three structures, there is a different sequence of line segment lengths. In the CdBi₂S₄ structure, for example, the line segments alternate between those which contain three metal atoms and those which contain five. Following the notation of Hyde et al., we call this structure a (5, 3) structure.^{1b} Examination of the CdBi₄S₇ and Cd_{2.8}Bi_{8.1}S₁₅ structures shows that these are respectively (4, 3) and (5, 3, 4, 3) structures. The (5, 3, 4, 3) Cd_{2.8}Bi_{8.1}S₁₅ structure is therefore an intergrowth of the (4, 3) CdBi₄S₇ and the (5, 3) CdBi₂S₄ structure types.

Hyde and co-workers also pointed out that there is a direct correlation between the average length of each zig or zag line segment, n , and the ratio of metal-to-sulfur sites.^{1b} The general rule is that if m is the number of metal sites and s is the number of anion sites then $n = s/(s - m)$. This relation between m , s , and n demonstrates the direct relation between the number of defects in the original NaCl cell, $(s - m)/s$, and the number of tilt planes. No defects are found in high-pressure CdS phase, which crystallizes in a NaCl cell (for which $n = \infty$). The other extreme is Bi₂S₃ where the average zigzag line segment length is 3 and $(s - m)/s = 0.333$, i.e., one-third of the original NaCl sites have been removed. From this general rule, we could also derive the relation between n and the average oxidation state of cations, q , using the charge balance condition

$$n = s/(s - m) = 2(s/m)/[2(s/m) - 2] = q/(q - 2)$$

where $q = 2(s/m) = (2m_{\text{Cd}} + 3m_{\text{Bi}})/(m_{\text{Cd}} + m_{\text{Bi}})$. Cd and Bi are assumed to be respectively in the +2 and +3 oxidation state. In the CdBi₂S₄ structure, for example, q is 8/3 (1 Cd²⁺ and 2 Bi³⁺) and therefore the calculated n is 4. In Table 6 we calculated n values for four Cd–Bi–S phases from q values and directly compared those n values to observed ones. As may be seen the agreement between the two columns is very good. These latter results demonstrate that the number and types of the metal cations, in other words the average oxidation state of the cations, do explicitly control the number of twinning planes even in the presence of metal disorders.

We may use these analyses to partially deduce the structure of the Cd₂Bi₆S₁₁ phase for which we found only one single crystal of insufficient quality for a full structural analysis. As Table 6 shows, the calculated n value is 3.68 or roughly three and two-thirds. Assuming that no individual n value will be smaller than 3, the only sequences of zigzag lengths compatible with the observed monoclinic unit cell are (5, 3, 4, 3, 4, 3), (5, 4, 3, 3, 3, 4), (3, 3, 5, 3, 5, 3), and (7, 3, 3, 3, 3, 3).⁹ Of these chain sequences the (5, 3, 4, 3, 4, 3) may be seen to be an intergrowth of the (5, 3, 4, 3) Cd_{2.8}Bi_{8.1}S₁₅ and the (4, 3) CdBi₄S₇ structures. As we have a detailed knowledge of the atomic positions in Cd_{2.8}Bi_{8.1}S₁₅ structure, we can use our knowledge of these positions to replicate the (4, 3) sequence in Cd_{2.8}Bi_{8.1}S₁₅ to construct a (5, 3, 4, 3, 4, 3) cell. Such a calculated cell has dimensions of $a = 13.111$ Å, $b = 3.989$ Å, $c = 35.87$ Å, and $\beta = 90.44^\circ$. These compare well with observed axes of $a = 13.112$ Å, $b = 3.997$ Å, $c = 35.84$ Å, and $\beta = 90.39^\circ$. These results suggest (but do not prove) that the Cd₂Bi₆S₁₁ structure may well be another intergrowth of CdBi₂S₄ and CdBi₄S₇.¹¹

The structural data of the previous section are particularly of interest with respect to chemical segregation. By segregation we mean the disproportionation of certain elements toward the twinning plane. There are three different NaCl sheet types in the CdBi₂S₄ and Cd_{2.8}Bi_{8.1}S₁₅ structures. In the CdBi₂S₄ structure we have narrow NaCl slabs for which there are $n = 3$ line segments and wider slabs that have $n = 5$ segments. In Cd_{2.8}Bi_{8.1}S₁₅, we have $n = 3$, $n = 4$, and $n = 5$ NaCl ribbons. For the $n = 3$, $n = 4$, and $n = 5$ sheets there are respectively two, two, and three crystallographically inequivalent metal sites. We turn first to the $n = 3$ sheets. For this sheet we find, for both CdBi₂S₄ and Cd_{2.8}Bi_{8.1}S₁₅ cases, complete segregation between the inner and outer sites. The outer site is a pure bismuth site while the interior site is purely occupied by cadmium atoms.¹⁰ In the case of the larger $n = 5$ segments of CdBi₂S₄, the outermost, the intermediate, and the innermost metal sites have respectively 100% Bi/0% Cd, 82% Bi/18% Cd, and 40% Bi/60% Cd. A fairly similar picture emerges for the $n = 5$ segment of Cd_{2.8}Bi_{8.1}S₁₅ where the mix at the three sites of the $n = 5$ sheet are respectively 100% Bi/0% Cd, 86% Bi/13% Cd, and 40% Bi/60% Cd. Finally for the $n = 4$ sheet, no segregation occurs as all sites are completely occupied by bismuth atoms. In both $n = 3$ and $n = 5$ sheet types we see a clear progression from a pure Bi site at the exterior of the sheet to more cadmium-rich sites in the interior. This trend can be understood from simple packing considerations. The NaCl structure contains a closest packing of both cation and anion sites. At the tilt planes one breaks open this closest packing. There is therefore

(9) Other permutations of the various n values which also lead to acceptable orthorhombic cells are (4, 3, 4, 4, 3, 4), (4, 4, 3, 3, 4, 4), (3, 5, 3, 3, 5, 3), and (3, 3, 5, 5, 3, 3).

(10) These results are also compatible with our best-fit powder pattern for the (4, 3) CdBi₄S₇ in which of the three sites two are purely occupied by Bi and the remaining third site is purely cadmium. This corresponds to the interior site of the $n = 3$ slab being purely cadmium and the exterior site of $n = 3$ being purely bismuth. Both interior and outer sites of the $n = 4$ sheet are pure bismuth sites. We see therefore for both the $n = 3$ and $n = 4$ sheets a picture similar to that found in CdBi₂S₄ and Cd_{2.8}Bi_{8.1}S₁₅.

(11) Similar intergrowth patterns have been found in Mn₂Er₆S₁₁ and Tm₈S₁₁. Both compounds show the (4, 3, 4, 4, 3, 4) cell. See ref 1j and for Tm₈S₁₁: Zhang, Y.; Franzen, H. F.; Harbrecht, B. *J. Less-Common Met.* **1990**, *166*, 135.

more room at the twinning planes. Evidence of this greater room is in the higher potential coordination number of the metal site at the twinning planes, which without distortion could be a nine-coordinate tricapped trigonal prism, a much larger site than the regular six-coordinate octahedral coordination of the NaCl structure.¹² The larger bismuth atoms therefore migrate to the grain boundary to take advantage of the greater space. By contrast, it appears difficult to deduce the amount of cadmium occupation in the interior of the slabs. Among the three sheet types described in this paper we vary from complete occupation of the interior by cadmium (for $n = 3$), to partial occupation (for $n = 5$) to no occupation (for $n = 4$).

(12) Examples of ions which take advantage of this higher potential coordination number are the metal atoms in the structures of (9, 9) heyrovskyite, (9, 6) vikingite and the (3, 3) NdYbS₃ where the larger metals occupy bicapped trigonal prismatic sites. See ref 3 and for NdYbS₃: Carré, D.; LaRuelle, P. *Acta Crystallogr.* **1974**, B30, 952.

Acknowledgment. The authors are grateful for the assistance of Carl Henderson of the University of Michigan Electron Microbeam Analysis Laboratory, Ted J. Huston of the University of Michigan Elemental Analysis Laboratory, and Dr. Jeff Kampf of the University of Michigan Chemistry Department for collection and discussion of single-crystal X-ray data sets. This research was supported by the Petroleum Research Fund administered by the American Chemical Society. We thank the A. P. Sloan Foundation and the J. D. and C. T. MacArthur foundations for fellowships granted to S.L.

Supporting Information Available: Tables of crystallographic data (9 pages); tables of structure factors (11 pages). Ordering information is given on any current masthead page.

CM9703841